S1 Field data and gravity corrections

Below, a summary of the gravity survey field data and associated corrections are provided. Table S1 provides the raw gravity data, as well as important spatial information associated with each data point. Table S2 provides the calculated corrections, with an in depth explanation of the associated equations given in Sect. S2. Figure S1 plots the influences associated with the solid Earth tides over the extent of the survey periods.

Table S1. Gravity survey field data recorded on 10 October 2022 and 1 September 2023 for each point across Comox (left) and Kokanee (right) Glacier respectively. Control measurements made before each survey (av.) on 8 October 2022 and 30 August 2023, and after each survey (ap.) on 11 October 2022 and 4 September 2023 are listed below. The recorded gravitational value (mGal), time of measurement (PST), altitude (Alt.), North and West coordinates (N/W), relative height (Ht.), and distance (Dst.) to the point 1 base station are provided. Since the control measurements were located in Victoria, BC at the same location, and only compared against each other, positional data relative to the CG and KG base stations have been omitted.

Comox Glacier							Kokanee Glacier						
#	mGal ±0.05	*PST*	*Alt.*(m) ±5	*N/W* ±0.00005	*Ht.*(m) ±0.05	*Dst.*(m) ±0.1	#	mGal ±0.05	*PST*	*Alt.*(m) ±5	*N/W* ±0.00005	*Ht.*(m) ±0.05	*Dst.*(m) ±0.1
1	4266.73	12:01	1880	$^{49.54586}/_{-125.35709}$	0.00	0.0	1	3990.29	13:20	2661	$^{49.74992}/_{-117.14843}$	0.00	0.0
2	4266.52	12:12	1879	$^{49.54617}/_{-125.35698}$	-0.93	37.4	2	3987.74	13:34	2659	$^{49.74986}/_{-117.14814}$	-1.13	25.9
3	4267.04	12:26	1875	$^{49.54662}/_{-125.35704}$	-5.22	84.5	3	3986.93	13:41	2659	$^{49.74976}/_{-117.14778}$	-1.41	52.3
4	4267.61	12:35	1874	$^{49.54694}/_{-125.35701}$	-5.98	120.2	4	3986.68	13:47	2658	$^{49.74971}/_{-117.14754}$	-2.11	70.4
5	4267.90	13:06	1868	$^{49.54726}/_{-125.35697}$	-12.33	155.9	5	3986.145	13:53	2659	$^{49.74966}/_{-117.14723}$	-1.53	88.8
6	4267.12	13:15	1869	$^{49.54767}/_{-125.35723}$	-11.48	201.5	6	3985.68	14:03	2658	$^{49.74959}/_{-117.14697}$	-2.41	110.2
7	4267.33	13:21	1868	$^{49.54831}/_{-125.3575}$	-11.67	274.0	7	3985.6	14:12	2657	$^{49.74955}/_{-117.14671}$	-3.09	129.4
8	4266.92	13:26	1869	$^{49.54887}/_{-125.35764}$	-10.76	337.4	8	3984.93	14:20	2658	$^{49.74938}/_{-117.14642}$	-2.63	159.4
9	4266.93	13:33	1868	$^{49.54925}/_{-125.35768}$	-11.55	409.2	9	3984.36	14:25	2660	$^{49.74929}/_{-117.14602}$	-0.78	187.6
10	4267.78	13:42	1866	$^{49.5498}/_{-125.35726}$	-14.07	438.3	10	3984.05	14:32	2661	$^{49.74921}/_{-117.14555}$	0.20	224.1
11	4267.12	13:49	1870	$^{49.54983}/_{-125.35796}$	-9.80	445.9	11	3987.39	14:41	2661	$^{49.74992}/_{-117.14843}$	0.00	0.0
12	4269.71	14:18	1880	$^{49.54586}/_{-125.35709}$	0.00	0.0	-	-	-	-	-	-	-
av.	4575.63	22:27	-	$^{48.46341}/_{-123.28809}$	-	-	av.	4578.96	0:20	-	$^{48.46341}/_{-123.28809}$	-	-
ap.	4575.88	19:16	-	$^{48.46341}/_{-123.28809}$	-	-	ap.	4579.23	22:21	-	$^{48.46341}/_{-123.28809}$	-	-

S2 Gravity data reduction

Following collection of the relative gravity survey data (Table S1), it is necessary to make a series of corrections (Table S2) in order to isolate the contribution sourced only from the local subsurface density structure (δg^{boug}). The local Bouguer gravity anomaly is then modelled to enable determination of the glacier ice thickness. This section includes an explanation and description of each gravity data correction used in Table S2, in the order in which they are applied to the raw data (g^{obs}). That is:

$$\delta g^{boug} = g^{obs} + \Delta g^{tide} - \Delta g^{base} - \Delta g^{drift} \pm \Delta g^{lat.} + \Delta g^{top.} - \Delta g^{bp} + \Delta g^{elev.} \tag{S1}$$

all to be defined.

S2.1 Tidal correction, Δg^{tide}

Before any other corrections can be applied, the temporal changes in gravity caused by the dynamics of the Sun, Moon, and Earth must be accounted for (Lowrie and Fichtner, 2020). Minute to minute, the Sun and Moon will not only contribute a changing yet measurable difference in gravitational acceleration (such as the Moon acting against the downward acceleration of gravity when overhead), but also deform the Earth's surface. Similar to the ocean tides, by the variable pull from the celestial

Table S2. Comox (left) and Kokanee (right) Glacier gravitational anomaly corrections used to retrieve the Bouguer anomaly for each point over the two transects. The control measurements made before (*av.*) and after (*ap.*) each survey are additionally provided at the bottom. All listed values are in mGal.

	Comox Glacier							Kokanee Glacier					
#	Δg^{tide}	Δg^{drift}	$\Delta g^{lat.}$	$\Delta g^{elev.}$	Δg^{bp}	$\Delta g^{top.}$	#	Δg^{tide}	Δg^{drift}	$\Delta g^{lat.}$	$\Delta g^{elev.}$	Δg^{bp}	$\Delta g^{top.}$
	$\pm 2.E(-4)$	$\pm 2.4\%$	$\pm 1.\%$	$\pm 1.\%$	$\pm 5.6\%$	± 0.08		$\pm 2.E(-4)$	$\pm 2.4\%$	$\pm 1.\%$	$\pm 1.\%$	$\pm 3.1\%$	± 0.08
1	2.86*E*(-2)	0.0	0.0	0.0	0.0	0.0	1	-3.16*E*(-2)	0.0	0.0	0.0	0.0	0.0
2	2.23*E*(-2)	0.23	-2.77*E*(-2)	-0.287	0.113	-0.02	2	-3.83*E*(-2)	-0.51	-4.64*E*(-3)	-0.349	0.130	0.09
3	1.39*E*(-2)	0.53	-6.79*E*(-2)	-1.61	0.635	0.30	3	-4.13*E*(-2)	-0.76	-1.24*E*(-2)	-0.435	0.163	0.17
4	8.5*E*(-3)	0.72	-9.65*E*(-2)	-1.85	0.730	-0.11	4	-4.40*E*(-2)	-0.98	-1.62*E*(-2)	-0.651	0.243	0.15
5	-1.07*E*(-2)	1.38	-0.125	-3.81	1.50	0.01	5	-4.66*E*(-2)	-1.20	-2.01*E*(-2)	-0.472	0.176	0.02
6	-1.62*E*(-2)	1.57	-0.162	-3.54	1.40	-0.15	6	-5.10*E*(-2)	-1.56	-2.55*E*(-2)	-0.743	0.277	0.19
7	-1.98*E*(-2)	1.69	-0.219	-3.60	1.42	0.16	7	-5.47*E*(-2)	-1.88	-2.86*E*(-2)	-0.954	0.356	0.22
8	-2.26*E*(-2)	1.80	-2.69*E*(-2)	-3.32	1.31	0.75	8	-5.77*E*(-2)	-2.17	-4.18*E*(-2)	-0.812	0.303	0.23
9	-2.68*E*(-2)	1.95	-0.303	-3.56	1.40	0.55	9	-5.98*E*(-2)	-2.35	-4.82*E*(-2)	-0.241	8.99*E*(-2)	0.28
10	-3.19*E*(-2)	2.14	-0.352	-4.34	1.71	0.41	10	-6.21*E*(-2)	-2.61	-5.47*E*(-2)	6.17*E*(-2)	-2.31*E*(-2)	0.29
11	-3.59*E*(-2)	2.29	-0.354	-3.02	1.19	0.44	11	-6.52*E*(-2)	-2.93	0.0	0.0	0.0	0.0
12	-5.08*E*(-2)	2.90	0.0	0.0	0.0	0.0	-	-	-	-	-	-	-
av.	-2.02*E*(-2)	-	-	-	-	-	- av.	-6.09*E*(-3)	-	-	-	-	-
ap.	-6.55*E*(-2)	-	-	-	-	-	- ap.	-5.08*E*(-2)	-	-	-	-	-

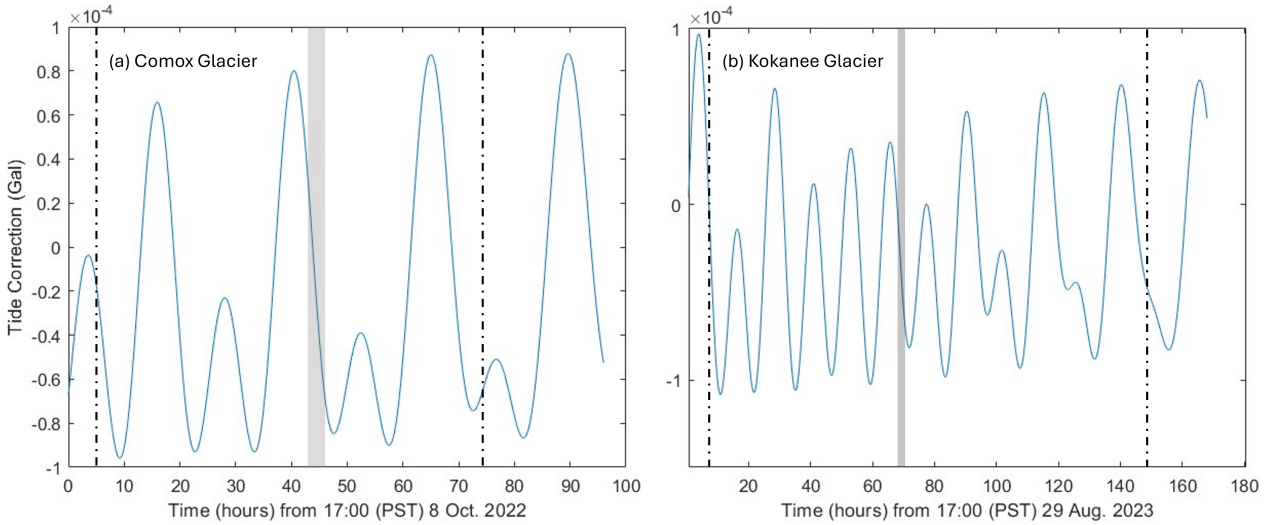

Figure S1. Calculated corrections for the gravity effect of solid Earth tides for Comox Glacier (a) and Kokanee Glacier (b) during the survey periods on each glacier (shaded areas) and control measurements in Victoria, BC (dashed lines).

bodies and the rotation of the Earth, the Earth's crust will gain a small ellipsoid form (i.e. solid Earth tides). These can be expected to reach up to 0.15 mGal.

Fortunately, with the tidal equations being well studied for over a millennium, a MATLAB code, adopted from a program formulated by Ahern (1993) and based on Schureman (1924) and Longman (1959), was provided by Samantha Palmer (personal communication, 2016) to perform the set of relevant calculations. The resulting tide correction determined over the time period of each survey may be seen in Fig. S1.

S2.1.1 Control measurement results

To ensure consistency and that the apparatus was undamaged for the experiment, control measurements were taken at the same location in Victoria, BC before and after each survey. Although some minor changes in the observed gravity are expected due to thermal fluctuations within the internal components of the gravity meter, over this time the tidal changes will provide the greatest influence. Values of 4688.61 and 4688.81 mGal are obtained before and after the CG survey, as well as 4692.05 and 4692.27 mGal for the KG survey.

With a difference of approximately 5*E*(-3)% or 0.2 mGal before and after in each case, and acknowledging that the internal influences are incalculable here, it is assumed that this result indicates that the gravity meter was not damaged, and maintained working order throughout the surveys.

S2.2 Relative adjustment and instrument effects, Δg^{base} & Δg^{drift}

At the start of the survey a base location must be chosen from which to compare all future relative measurements against. At this location, regardless of time or relation to the rest of the survey area, δg^{boug} will be defined as 0 mgal. Taking a measurement at this location g^{base} therefore sets the value which must be subtracted from all future observations (i.e. Δg^{base}) (LaCoste & Romberg, 1989).

Influences internal to the gravity meter must also be considered. To seclude it from the environment the internal mechanism of the gravity meter is housed inside an airtight thermostatic case, kept at a temperature above (most) external environments at 51 °C (LaCoste & Romberg, 1989). Due to the natural material properties of the spring, specifically the thermal expansion coefficient, a small drift in the measured values will be present over the course of an experiment, Δg^{drift}. For this reason measurements must be made at the base location at the start and end of the survey, giving a total measurement drift of Δg^{diff}. While some longer or varied surveys require corrections necessitating polynomial or numerically determined functions of the drift (Elsaka, 2020), here the induced changes are assumed to be a linear function with time t over full survey time Δt, thus giving a point-to-point drift correction of:

$$\Delta g^{drift} = \frac{t}{\Delta t}\Delta g^{diff} \tag{S2}$$

S2.3 Latitude correction, $\pm\Delta g^{lat.}$

With the solid Earth tides corrected for and a zero point set at the base station, corrections associated with the latitude and elevation, as well as surrounding terrain, need to be determined. It is first noted that Earth is not a sphere, but an ellipsoid bulging at the equator (Lowrie and Fichtner, 2020). Let $f = (a-c)/a$ be the flattening of the ellipsoid about the poles where a and c are the major and minor axis, respectively. Let it also be given that A is the ratio of the ellipsoid equatorial centrifugal acceleration caused by Earth's rotation to the equatorial gravitational acceleration. The gravity normal to the surface of an ellipsoid at some angle (latitude), $g^{lat.}$, is (Lowrie and Fichtner, 2020)

$$g_n = g_e(1 + C_1 \sin^2\phi + C_2 \sin^2 2\phi) \tag{S3}$$

where g_e is the mean equatorial gravity around the major axis, ϕ is the angle from the equator, and C_1, C_2 are

$$\begin{aligned} C_1 &\approx \frac{5}{2}f - f + \frac{15}{4}A^2 - \frac{27}{14}fA \\ C_2 &\approx \frac{1}{8}f^2 - \frac{5}{8}fA \end{aligned} \tag{S4}$$

For Earth, g_e is $978,031.85$ mGal, and C_1 reduces to around $0.005278895/R_e$ with $R_e = (a^2c)^{1/3} = 6371\mathrm{km}$. Since C_2 is composed of only higher order fA and f^2 terms it follows that $C_2 \ll C_1$ so may be neglected here.

Taking the first derivative with respect to the angle, and some simple algebra, it is found that

$$g^{lat.} = g_e C_1 \sin(2\phi) \tag{S5}$$

Or, relative to some other latitude this is reformed to give

$$\Delta g^{lat.} = \frac{g_e \alpha}{R_E} \sin(2\phi) \Delta s \tag{S6}$$

where Δs is the north-south distance from the base station. The latitude correction from base station to measurement point has therefore been found. It is noted, though, that it must be taken relative to the base station, subtracting the value from the observed gravity for more northern measurements and adding it for more southern ones.

S2.4 Terrain and the Bouguer plate correction, $\Delta g^{top.}$ & Δg^{bp}

Local influences to gravity must also be considered. The following arguments are drawn from Lowrie and Fichtner (2020) and Cella (2015). Both a large valley (mass deficit) and mountain (mass "above" the measurement point) will work to decrease the observed gravity. One way to correct for this is as follows. By first looking at a straight line of terrain extending from the measurement point, one may divide it into sections of distance $r_1 < r_2 < \cdots < r_n$. One can then imagine wrapping the terrain around the measurement point to give it cylindrical symmetry. For example, if the line of terrain was up a hill, the measurement point would now sit at the bottom of a cone made of concentric rings of radius r_n.

A volume of rock with density ρ may then be considered from one of the cylinders at height z, radius r, and angle θ from the origin (measurement point). The mass contribution is thus $\mathrm{d}m = \rho r \mathrm{d}r\ \mathrm{d}z\ \mathrm{d}\phi$ for some amount of angle $\phi_1 \to \phi_2$ around the cylinder. The contribution of gravity from this point is

$$g_n = G \frac{\mathrm{d}m}{r^2 + z^2} \cos\theta = G \frac{\rho r z \mathrm{d}r\ \mathrm{d}z\ \mathrm{d}\phi}{(r^2 + z^2)^{3/2}} \tag{S7}$$

where G is the gravitational constant. This can then be integrated over the volume to get the contribution at the measurement point

$$g = G\rho \int_{\phi_1}^{\phi_2} \mathrm{d}\phi \int_{r_n}^{r_n+1} \int_{z=0}^{z+h} \frac{rz}{(r^2 + z^2)^{3/2}} \mathrm{d}z\ \mathrm{d}r \tag{S8}$$

This integral must be taken for every volume element, over every cylinder, at every location measured to retrieve $\Delta g^{top.}$. Fortunately, code already exists to complete these corrections. Here, GTeC software is used (Cella, 2015). Similar to above, the code looks at partitioned concentric rings around the measurement point. Input to these calculations was a 1:20,000 topographic dataset at a pixel size of 2 m and elevation grid of 25 m provided by GeoBC (2013).

With the terrain correction complete, the valley or peak surrounding the measurement may be considered filled in or removed. However, the measurement point is now sitting on top of or below a uniform fictitious layer of rock relative to the base station. The Bouguer plate correction is therefore introduced where the contribution is removed as (Lowrie and Fichtner, 2020)

$$\Delta g^{bp} = 2\pi G \rho h \tag{S9}$$

where h here is the thickness of the fictitious layer (elevation difference) compared to the base station. With this, all points now sit in the free air suspended above a perfect ellipsoid of mass m_e.

S2.5 Elevation (free air) correction, $\Delta g^{elev.}$

As a simple final correction, the elevation correction works to account for differences in gravity caused by getting farther from the Earth (or a perfect ellipsoid when the other corrections are applied), here taken as a point mass. That is (Lowrie and Fichtner, 2020)

$$g^{elev.} = \frac{\mathrm{d}}{\mathrm{d}r} \left(-\frac{G m_e}{r^2} \right) = \frac{2 g_e}{r} \tag{S10}$$

where m_e is the mass of Earth. The correction relative to a base station is thus

$$\Delta g^{elev.} = \frac{2g_e}{r}\Delta h \tag{S11}$$

where Δh is the change in height.

References

Ahern, J. L.: A program for calculating the tidal acceleration due to the Moon and Sun, available at http://gravmag.ou.edu/reduce/tide-acd.txt, 1993.

Cella, F.: GTeC—A versatile MATLAB® tool for a detailed computation of the terrain correction and Bouguer gravity anomalies, Compute. & Geosci., 84, 72-85, https://doi.org/10.1016/j.cageo.2015.07.015, 2015.

Elsaka, B.: Comparison of different polynomial degrees for correcting the instrumental drift of Scintrex CG-5 Autograv Gravimeter, Aust. J. Basic Appl. Sci., 14, 19-25, https://doi.org/10.22587/ajbas.2020.14.5.3, 2020.

GeoBC: Topographic Maps (1:20,000), British Columbia Ministry of Energy, Mines and Petroleum Resources Mining and Minerals Division, https://pub.data.gov.bc.ca/datasets/177864/ [data set], 2013.

LaCoste & Romberg, Inc., LaCoste & Romberg: Instruction manual for LaCoste & Romberg, Inc. model G and D land gravity meter, Austin Texas, USA, 1989.

Longman, I.: Formulas for computing the tidal accelerations due to the moon and the sun, J. Geophys. Res., 64, 2351-2355, https://doi.org/10.1029/JZ064i012p02351, 1959.

Lowrie, W., Fichtner, A.: Fundamentals of Geophysics, 3, Cambridge University Press, 10.1017/9781108685917, 2020.

Schureman, P.: Manual of harmonic analysis and prediction of tides [revised 1941 and 1958], US Coast and Geodetic Survey; special publication 98, United States Government Printing Office, Washington DC, USA, https://doi.org/10.25607/OBP-155, 1924.